

# The monotectic reaction in Cu-Nb alloys

J. D. VERHOEVEN, E. D. GIBSON

*Ames Laboratory-DOE and Department of Materials Science and Engineering, Iowa State University, Ames, Iowa 50011, USA*

The solidification of Cu–Nb alloys has been studied by a chill casting technique. Formation of small spherical particles, termed spheroids, was observed at compositions of 15 and 20 wt % Nb, and comparison to similar particles found in chill cast Cu–Pb alloys presents evidence that the spheroids are produced by a monotectic reaction. It is shown that the spheroids are induced by oxygen impurities in the alloys and that their formation is also promoted by high solidification rates. A mechanism for spheroid formation is postulated.

## 1. Introduction

In recent years there has been a strong interest in the superconducting properties of binary Cu–Nb alloys prepared by solidification from the melt [1–7]. In all of these studies the superconducting properties will be strongly influenced by the microstructure of the Nb phase in the Cu–Nb alloys. The binary Nb–Cu phase diagram would be extremely useful in understanding and predicting the microstructure of these alloys. At the present time there are two proposed Nb–Cu phase diagrams in the literature, as shown on Fig. 1. The study of Popov and Shiryayeva [8] indicates a

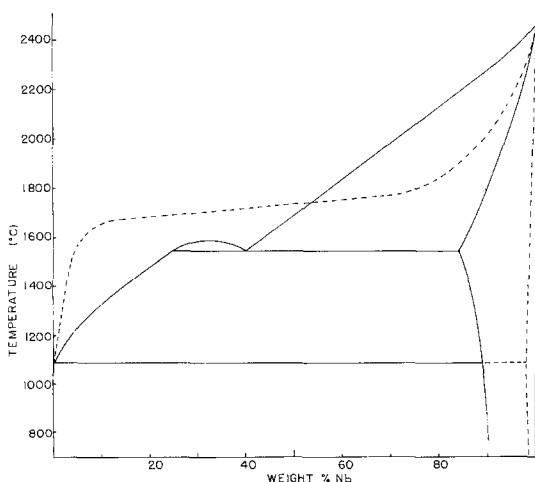


Figure 1 Copper–niobium phase diagrams proposed by Allibert *et al.* [9], dashed lines, and by Popov *et al.* [8], solid lines.

liquid state immiscibility with a monotectic reaction, whereas the study of Allibert *et al.* [9] indicates a nearly horizontal liquidus but not immiscibility. Based on the lack of metallographic evidence by Popov the presence of the monotectic reaction has been questioned [10], and it generally assumed [11] that the diagram of Allibert *et al.* is more nearly correct. This conclusion is also supported by the unpublished M.S. thesis of Schelle [12].

The present study offers evidence to show that a monotectic reaction does occur in Cu–Nb alloys, but that it is induced by oxygen impurities.

## 2. Experimental technique

The alloys were prepared by a chill casting technique. A 4 mm hole was drilled into the bottom centre of a 25 mm diameter crucible. Then a 6 mm diameter closed-end tube of the same material as the crucible was inserted into this hole from above to act as a plug. This tube contained a W/W-26 Re thermocouple down its centre which was used to measure the melt temperature. The thermocouple was calibrated against the melting point of platinum. Pure Nb and Cu were placed in the crucible and heated under a vacuum of around  $10^{-5}$  torr by a 450 kc induction coil which induced heating currents into a Ta susceptor surrounding the crucible. After the Cu melted, argon was introduced to a pressure of 100 mm vacuum and the melt was held at between 1850 and 1880°C for 5 min prior to casting. The melt was cast by raising the tube plug which allowed the melt to drain into a 13 mm diameter Cu mould which was chilled by flowing

water. The melts were 75 g in weight and produced an ingot of around 4.4 cm height. The ingots were sectioned at various positions and prepared for examination by standard metallographic polishing techniques. The surfaces were etched by a 5 sec immersion in a solution of 55/25/20 phosphoric, acetic and nitric acids. This treatment removed the Cu phase with no noticeable effect upon the Nb phase. The samples were then examined by optical and scanning electron microscopy.

### 3. Experimental results

Initial experiments were carried out using crucibles of  $\text{Al}_2\text{O}_3$  and crucibles of  $\text{ZrO}_2$  stabilized with CaO. The starting metals were Cu of 99.999+ purity and Nb of 99.92+ purity. Alloys of 40 wt% Nb cast from both types of crucibles were observed to have uniform distribution of fine Nb dendrites in a Cu matrix, as shown in Fig. 2. However, when the composition was changed to both 15 and 20 wt% Nb the chill cast structure displayed an array of circular particles among the Nb dendrites as shown in Fig. 3. These circular particles were distributed fairly uniformly throughout the casting. Deep etching and examination in the scanning electron microscope (see Fig. 4) revealed that these circular particles were spherical rather than cylindrical, and hence they will be termed spheroids. They are composed of an outer shell of Nb and an interior which is a two-phase mixture of Cu and Nb.

In order to reveal the role of impurities in producing these spheroids a rather complete chemical analysis was carried out on samples cast from both  $\text{Al}_2\text{O}_3$  and CaO-stabilized  $\text{ZrO}_2$  crucibles. Analyses were made for all elements of the periodic table

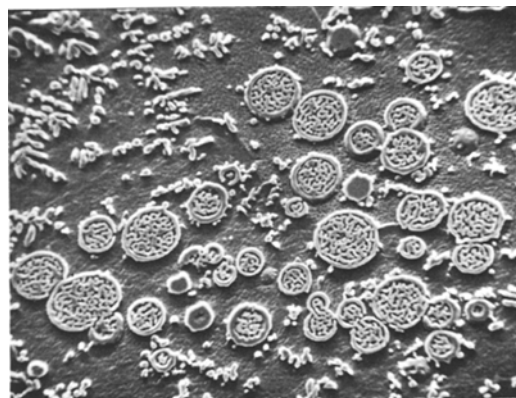


Figure 3 Microstructure of a 20 wt% Nb-Cu alloy chill cast from a  $\text{ZrO}_2$  (CaO) crucible using conditions identical to Fig. 2 ( $\times 700$ ).

using spark source mass spectroscopy. To obtain more quantitative results on O, N, and H the vacuum fusion technique was employed, and on C the combustion technique was employed. Analysis of both the pure Cu and Nb were made and these analyses, weighted for a 20 wt% Nb alloy (14.6 at. %), are included in Table I under the column headed "Starting metals". Therefore, direct comparison with this column reveals which impurities were in the original metals and which were picked up during alloy preparation. The vacuum fusion analyses and combustion analyses are both good to around  $\pm 5\%$  but the mass spectrometer analyses are semiquantitative and differences are significant only when they are larger than a factor of around 2 to 3 or more.

It was apparent that there was some attack of the  $\text{Al}_2\text{O}_3$  crucibles because about 0.2 to 0.4 mm of ceramic material was removed where the melt

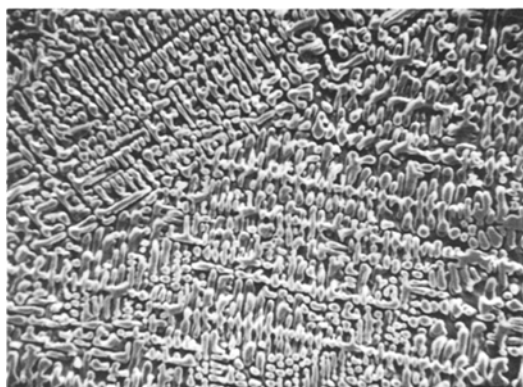


Figure 2 Microstructure of a 40 wt% alloy chill cast from a  $\text{ZrO}_2$  (CaO) crucible at 1850 to 1880° C ( $\times 700$ ).

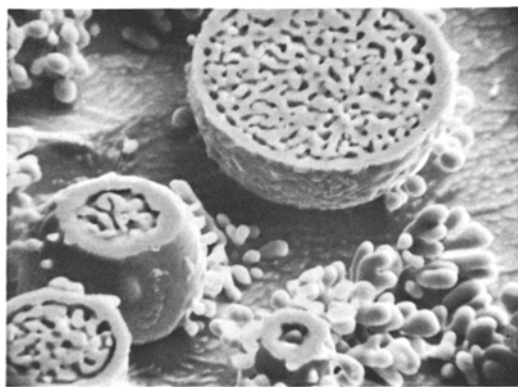


Figure 4 Structure of spheroids revealed by deep etching away the Cu phase ( $\times 2450$ ).

TABLE I Chemical analyses of chill cast 20 wt% alloys where spheroids were present throughout the casting (all analyses are p.p.m. atomic except H which is p.p.m. weight)

Element	Crucible			Starting metals <sup>(b)</sup>
	Al <sub>2</sub> O <sub>3</sub> <sup>(a)</sup>	ZrO <sub>2</sub> (CaO) <sup>(a)</sup>	ZrO <sub>2</sub> (CaO) <sup>(a)</sup>	
O	16 000	4600	3000	180
N	62	19	87	89
H	11	7	—	24
C	67	45	—	63
B	8	2	—	4
Na	3	6	—	1
Mg	37	60	—	4
Al	1 000	40	—	3
Si	210	100	—	66
S	4	2	—	1
Cl	0.7	2	—	1
K	3	4	—	1
Ca	30	20	—	1
Ti	1	4.2	—	0.1
Fe	10	10	—	20
Zr	10	87	—	1
In	3.9	<.03	—	<0.1
Sn	67	0.1	—	<0.4
Mo	<1	3	—	<2
Ta	73	200	—	140
W	3	10	—	5

(a) High purity crucibles purchased from Ventron Corp.

(b) Cu purchased from Asarco Inc., and Nb from Wah Chang Corp.

made contact. This attack is also revealed by the high O and Al contents found in Table I. For the ZrO<sub>2</sub> (CaO) crucibles no apparent removal of ceramic material from the crucible wall was evident, but a colour change occurred at the metal/ceramic contact surfaces. The colour change became progressively less going into the ceramic wall. This result indicates a stoichiometry change. The analyses of Table I show a significant pickup of O and very little pickup of Zr, thus indicating that the liquid alloy does not remove Zr atoms from their lattice but does leach out O atoms, which is consistent with a stoichiometry change.

Examination of the data of Table I reveals that if any impurity is inducing the spheroid formation it is most probably O. The oxygen could be coming from either the crucible itself, as postulated above, or from the argon. Therefore two additional experiments were done on ZrO<sub>2</sub> (CaO) crucibles using ultra-pure argon and also using zone-refined Cu and Nb (O content weighted for 20% alloy was 87 p.p.m. Spheroids were found in both experiments and the O analyses were 3600 and 3800 p.p.m. atomic, thus indicating the O pickup was from the ZrO<sub>2</sub> (CaO) crucibles.

Experiments were then done using the zone-

refined Cu and Nb and the high purity argon with two new crucible materials, ZrO<sub>2</sub> stabilized with Y<sub>2</sub>O<sub>3</sub> and Y<sub>2</sub>O<sub>3</sub>. Chill castings from these crucibles displayed a uniform distribution of fine Nb dendrites throughout their interior, as seen in Fig. 5. There was no evidence of spheroids in these castings except for a very thin layer at the chill wall where spheroids of 1 to 2 μm in diameter



Figure 5 Microstructure of a 20 wt% Nb-Cu alloy chill cast from a Y<sub>2</sub>O<sub>3</sub> crucible under conditions identical to Fig. 3 (× 700).

TABLE II Chemical analyses of chill cast 20 wt% alloys where spheroids were absent from the bulk of the castings (all analyses are p.p.m. atomic except H which is p.p.m. weight)

Element	Crucible			Starting metals <sup>(d)</sup>
	ZrO <sub>2</sub> (Y <sub>2</sub> O <sub>3</sub> ) <sup>(a)</sup>	ZrO <sub>2</sub> (Y <sub>2</sub> O <sub>3</sub> ) <sup>(b)</sup>	Y <sub>2</sub> O <sub>3</sub> <sup>(c)</sup>	
O	2300	2100	760	87
N	29	19	34	24
H	6	6	5	1
C	57	96	62	37
B	3	3	20	0.6
Na	<3	2	3	<0.6
Mg	8.6	4	2.2	<0.02
Al	30	100	10	<0.3
Si	40	20	11	49
Cl	0.8	1	2	1
Ca	3	5	10	<1
Sc	3	1	<.09	<.05
Cr	1.8	0.7	0.4	<0.1
Fe	9.7	8.5	9.0	<3
Ni	6	0.9	1	<.2
Y	5.3	2.5	500	<.2
Zr	230	110	1	<.4
Ta	40	40	30	18

(a) Slip cast from ZrO<sub>2</sub>(Y<sub>2</sub>O<sub>3</sub>) powder purchased from Zircoa Corp.

(b) Purchased from Zircoa Corp.

(c) Slip cast from high purity Y<sub>2</sub>O<sub>3</sub> powder supplied by H. Burkholder, Ames Lab., DOE.

(d) Purchased from Materials Research Corp.

were mixed in with dendrites of 0.3 to 0.5  $\mu\text{m}$  stalk sizes. This result was consistently found in all three experiments shown in Table II. It may be seen that the oxygen content is lower than in the experiments of Table I where large spheroids (5 to 15  $\mu\text{m}$  diameter) were present throughout the castings. In addition, however, Mg, Si and Ca also appear to be lower with the Y<sub>2</sub>O<sub>3</sub> and ZrO<sub>2</sub>(Y<sub>2</sub>O<sub>3</sub>) crucibles and it is conceivable these elements could be responsible for the spheroid formation. Therefore, an additional experiment was carried out in which 2.4 wt% of Cu<sub>2</sub>O was melted with the zone-refined metals in a ZrO<sub>2</sub>(Y<sub>2</sub>O<sub>3</sub>) crucible similar to the one used for the alloy analysed in the second column of Table II. The Cu<sub>2</sub>O was prepared by air oxidation of high purity Cu sheet at 900° C. The blue colour of the oxide indicated it was all Cu<sub>2</sub>O rather than CuO. Analysis of the chill casting revealed an O level of 10 500 p.p.m. atomic, which is just slightly less than expected if all the O came from the Cu<sub>2</sub>O (the N analysis was 58 p.p.m.). Metallographic examination revealed spheroids in abundance throughout the casting. The impurity content of this casting should be the same as for the alloys whose analysis is given by the second column of Table II for all of the elements except O. The presence of spheroids in this last alloy and not in the alloy of Table II therefore offers strong

evidence that the spheroids are induced by O impurities rather than some other impurity.

In all of these experiments the crucibles did not empty completely and a small amount of alloy remained in the crucible. This remnant alloy solidified at a rate significantly lower than for the chill castings. After casting the power was simply turned off and the thermocouple remaining within the crucible just above the remnant alloy cooled to 1100° C in 50 to 60 sec. Spheroids were not observed in the remnant alloy remaining in the crucible except for the alloy containing 10 500 p.p.m. O. In this alloy large spheroids, 100 to 130  $\mu\text{m}$  diameter, were present in abundance within the small amount of remnant alloy. Hence, we have the following rate dependency. For alloys of low O level, 2300 p.p.m. and lower, spheroids only appear at the chill wall in the 1 to 2  $\mu\text{m}$  diameter size range. For alloys of intermediate O level, 3000 to 5000 p.p.m., spheroids appear throughout the chill casting in the 5 to 15  $\mu\text{m}$  diameter size range but not in the remnant alloy left in the crucible. For the alloy of high O level, 10 500 p.p.m., spheroids appear in the chill casting in the 5 to 15  $\mu\text{m}$  size range and are also present in the remnant alloy in the 100 to 130  $\mu\text{m}$  size range. It is clear that spheroid formation depends on both O content and solidification rate.

As regard the liquidus temperature one experiment was done on a 20 wt% Nb alloy where the melt was held at 1830 to 1850° C for 5 min and then cooled to 1730° C and cast from this temperature after a 40 sec hold. A very small but significant volume fraction of the casting contained distinctive primary Nb platelets which were never seen in the dozen or so castings poured from 1850 to 1880° C. Hence, it appears that the liquidus temperature at 20 wt% Nb is just slightly above 1730° C, which is even higher than the liquidus of Alliber *et al.* [9] and much higher than Popov and Shiryaeva [8].

The presence of spheroids suggests a monotectic reaction. However there is very little data available in the literature on chill cast monotectic alloys, although there are studies [13, 14] on Cu–Pb alloys which show some microstructures having similarities to the spheroids of Fig. 3. Therefore experiments were done on the Cu–Pb system which has a well characterized monotectic phase diagram. Chill castings were made at the two compositions shown on Fig. 6. The experimental arrangement was identical to that for the Nb–Cu experiments. The alloys were held for 3 min in graphite crucibles at a temperature roughly 200° C above the liquidus and then chill cast.

The microstructure of the 19.6 wt% alloy is shown in Fig. 7. The structure was fairly uniform throughout the casting and this picture is typical. The light phase is Cu and the dark phase Pb so that the spheroids consist of a Cu-rich shell surrounding an interior composed of a two-phase mixture of Pb and Cu. Note that the spheroid structures are very similar to those shown in Fig. 3 for the Nb–Cu

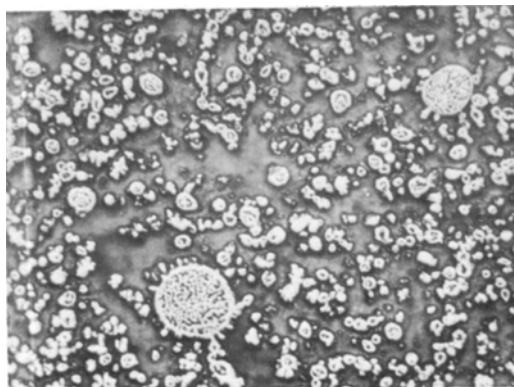


Figure 7 Microstructure of a chill cast 19.6 wt% Pb–Cu alloy (X 330).

alloys. In the Cu–Pb alloy of 36.9 wt% Cu a microscopic separation of the liquid into Pb-rich and Cu-rich liquid phases had occurred prior to solidification, in spite of the rapid quench. This fact was revealed by the microstructure which showed distinct Cu-rich and Pb-rich regions. These regions were elongated along the ingot axis and were radially symmetric, thus revealing the fluid flow pattern as the mould filled. The Cu-rich phase contained the Pb phase as a fine rod-like dispersion, very similar to the structures found by Livingston and Cline [15] in their study of directionally solidified Cu–Pb alloys of the monotectic composition. The Pb-rich phase contained spheroids throughout and appeared very similar to the microstructure of Fig. 7. Hence, it is seen that spheroid structures similar to those found in the Cu–Nb alloys form from the Pb-rich liquid phase of chill cast Cu–Pb alloys.

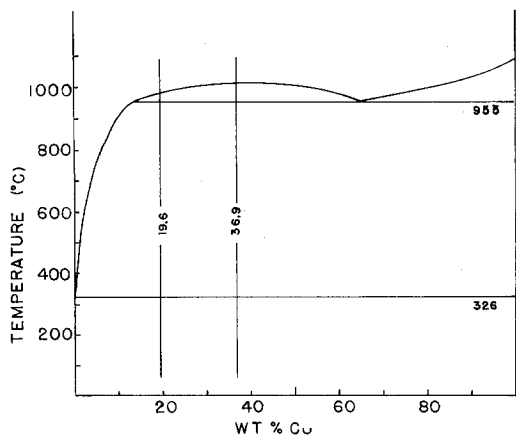


Figure 6 The Cu–Pb phase diagram showing composition of the alloys studied.

#### 4. Discussion

The spheroid formation in 15 and 20 wt% Nb alloys and the similarity of their microstructure to spheroids in Cu–Pb alloys presents strong evidence that monotectic solidification does occur in these Cu–Nb alloys at sufficiently high oxygen contents and solidification rates. For the chill castings poured from 1850 to 1880° C an O content of 3000 p.p.m. atomic is sufficient to produce the reaction in 20 wt% alloys. However, the reaction does not occur at this O impurity level if the cooling rate is as slow as occurred in the remnant alloy contained in the crucibles when the power was shut off.

These results offer a possible explanation for the discrepancy between the proposed phase diagrams of Popov and Shiryaeva [8] and Allibert *et*

*al.* [9]. It may be that the combination of O impurity level and cooling rate in Allibert's work was sufficiently low to avoid the monotectic reaction while in Popov's work it was not. Our experimental work supports the diagram of Allibert at 20 wt% Nb both with regard to the liquidus temperature and the absence of the monotectic reaction for equilibrium solidification at low oxygen impurity levels. At 40 wt% Nb we observe no metallographic evidence of a monotectic reaction even at O levels which show the reaction in 20 wt% alloys.

Details of the mode of formation of the spheroids will now be considered. In the Cu–Pb alloys it is clear that as soon as the Pb-rich liquid is cooled below its liquidus temperature formation of Cu-rich liquid will lower the free energy of the system. It is reasonable to assume that this Cu-rich liquid nucleates and grows into small spherical drops of liquid dispersed throughout the Pb-rich liquid during cooling prior to solidification. On further cooling the composition of the drops increases in Cu, approaching the monotectic composition. If the liquid drops supercool a bit below the monotectic temperature prior to nucleation of solidification, as seems likely, their composition would be enriched in Cu to the right of the monotectic composition shown on Fig. 6. It is then likely that solidification would nucleate by formation of the Cu phase at the surface of the drops. This would produce the rim of solidified Cu at the surface of the spheroid and drive the composition of interior liquid back toward the lower Cu composition of the monotectic. The latent heat liberated would raise the spheroid temperature back to nearer the monotectic temperature and the interior liquid would then solidify by the coupled growth of solid Cu and Pb-rich liquid at, or just below, the monotectic temperature, followed by solidification of the Pb-rich liquid on further cooling to 326° C.

The spheroids in the Cu–Nb alloys would be generated by the same mechanism, with their surface formed by nucleation of a Nb shell and their interior by coupled monotectic growth of solid Nb and liquid Cu. However, the question remains as to why the spheroid formation does not occur at slow cooling rates when it is observed at the higher cooling rates in the chill castings. Equilibrium solidification is more closely approached upon slow cooling and consequently, since spheroids are not observed on slow cooling one does not expect a monotectic reaction on the equilibrium phase

diagram, in agreement with the proposal by Allibert *et al.* in Fig. 1. Because of the nearly horizontal liquidus temperature one expects the free energy composition curve of the liquid phase,  $G_l$ , to be similar to the shape if a monotectic were present. As shown in Fig. 8, however, the dip in the curve at high compositions does not come down far enough to cause the monotectic liquid to be stable. On chill casting it is quite possible that the liquid phase will supercool somewhat. This means that on a diagram such as Fig. 8 the supercooled liquid phase will have a composition slightly higher than the equilibrium liquid phase, and will appear at a point such as A on Fig. 8. In this situation the free energy per mole to form a nucleus of Nb-rich liquid is shown by the length  $\Delta G_l$ , and that to form a nucleus of Nb-rich solid by length  $\Delta G_s$  [16]. Which phase forms depends upon which one may nucleate most easily. It is reasonable to assume that the liquid Nb phase will form first in spite of its smaller  $\Delta G$  of formation because nucleation barriers, such as surface interface energy, for the formation of a liquid nucleus are likely to be less than for a solid nucleus.

Hence, the rate dependency and the oxygen impurity dependency for formation of the spheroids observed in these experiments may be explained by the following argument. At lower cooling rates there is very small supercooling of the liquid and point A moves to the left on Fig. 8, thus causing  $\Delta G_l$  to go to zero and removing the driving force for nucleation of the liquid rich Nb phase. At increased oxygen levels the free energy composition curves are modified to increase the ratio of  $\Delta G_l$  to  $\Delta G_s$  either by a lowering of the dip

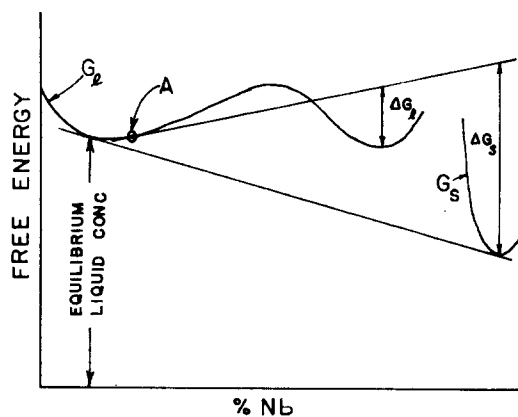


Figure 8 A possible equilibrium composition diagram for Cu–Nb alloys at temperatures between 1700 and 1100° C.

in the liquid curve,  $G_l$ , or by raising the solid Nb curve,  $G_s$ .

## 5. Summary

Chill casting experiments have been carried out on Nb–Cu alloys of 15, 20 and 40 wt % Nb. Formation of spheroid structures was observed in the 15 and 20 wt % alloys and comparison to similar structures observed in chill cast Cu–Pb alloys indicates that these structures form by a monotectic reaction. Further experiments have shown that the spheroid structures are induced by oxygen as an impurity in the alloys. The spheroid formation may be reduced or eliminated by lowering the O impurity level, and also by reducing the cooling rate. A possible kinetic mechanism to explain these effects is postulated. It is shown that oxygen pickup from  $Al_2O_3$  and  $ZrO_2$  (CaO) crucibles is larger than from either  $ZrO_2$  ( $Y_2O_3$ ) or  $Y_2O_3$  crucibles and that the  $Y_2O_3$  crucibles give the lowest oxygen contamination. The data obtained in this study support the equilibrium phase diagram proposed by Allibert [9] rather than that proposed by Popov [8].

## Acknowledgements

The authors would like to acknowledge the expert assistance of the following Ames Laboratory Personnel which made this study possible. The chemical analyses were done by Mr Robert Consemius, Mr Nile Beymer and Mr Robert Bachman. The slip cast crucibles were prepared by Mr Wayne Calderwood. The metallographic sample preparation was done by Mr Harlan Baker and he also developed the etching technique for us. The authors were assisted in the experimental work by Mr Thomas

Myers. Discussions of ceramic materials with Dr D. Wilder, Dr O. Hunter and Dr M. Berard were very helpful. This work was supported jointly by the Magnetic Fusion Energy Division and the Basic Energy Sciences Division of the United States Department of Energy.

## References

1. C. C. TSUEI, *Science* **180** (1973) 57.
2. C. C. TSUEI and L. R. NEWKIRK, *J. Mater. Sci.* **8** (1973) 1307.
3. C. C. TSUEI, *J. Appl. Phys.* **45** (1974) 1385.
4. R. ROBERGE and R. D. McCONNEL, *Scripta Met.* **8** (1974) 1267.
5. J. L. FIHEY, P. NGUYEN-DUY and R. ROBERGE, *J. Mater. Sci.* **11** (1976) 2307.
6. R. ROBERGE and J. L. FIHEY, *J. Appl. Phys.* **48** (1977) 1327.
7. A. DAS GUPTA, B. L. MORDIKE and L. SCHULTZ, *Mater. Sci. Eng.* **18** (1975) 137.
8. I. A. POPOV and N. V. SHIRYAEVA, *Russ. J. Inorg. Chem.* **6** (1961) 1184.
9. C. ALLIBERT, J. DRIOLE and E. BONNIER, *C. R. Acad. Sci., Paris 268C* (1969) 1579.
10. R. P. ELLIOTT, "Constitution of Binary Alloys", First supplement (McGraw-Hill Book Co., New York, 1965) p. 253.
11. "Metals Handbook", Vol. 8 (American Soc. Metals, Metals Park, Ohio, 1973) p. 281.
12. R. F. SCHELLE, M. S. Thesis, Iowa State University (1971).
13. E. PELZEL, *Metall.* **10** (1956) 1023.
14. S. OYA and A. KAMIO, *Nippon Kinzoku Gukkaishi* **33** (1969) 60.
15. J. D. LIVINGSTON and H. E. CLINE, *Trans. Met. Soc AIME* **2451** (1969) 351.
16. J. W. CHRISTIAN, "The Theory of Transformations in Metals and Alloys" (Pergamon Press, Oxford, 1965) p. 537.

Received 25 October and accepted 14 November 1977.